

Measurement of Azimuthal Asymmetries in Inclusive Charged Dipion Production in e^+e^- Annihilations at $\sqrt{s} = 3.65$ GeV

M. Ablikim,¹ M. N. Achasov,^{9f} X. C. Ai,¹ O. Albayrak,⁵ M. Albrecht,⁴ D. J. Ambrose,⁴⁴ A. Amoroso,^{49a,49c} F. F. An,¹ Q. An,^{46,a} J. Z. Bai,¹ R. Baldini Ferroli,^{20a} Y. Ban,³¹ D. W. Bennett,¹⁹ J. V. Bennett,⁵ M. Bertani,^{20a} D. Bettoni,^{21a} J. M. Bian,⁴³ F. Bianchi,^{49a,49c} E. Boger,^{23,d} I. Boyko,²³ R. A. Briere,⁵ H. Cai,⁵¹ X. Cai,^{1,a} O. Cakir,^{40a,b} A. Calcaterra,^{20a} G. F. Cao,¹ S. A. Cetin,^{40b} J. F. Chang,^{1,a} G. Chelkov,^{23,d,e} G. Chen,¹ H. S. Chen,¹ H. Y. Chen,² J. C. Chen,¹ M. L. Chen,^{1,a} S. J. Chen,²⁹ X. Chen,^{1,a} X. R. Chen,²⁶ Y. B. Chen,^{1,a} H. P. Cheng,¹⁷ X. K. Chu,³¹ G. Cibinetto,^{21a} H. L. Dai,^{1,a} J. P. Dai,³⁴ A. Dbeyssi,¹⁴ D. Dedovich,²³ Z. Y. Deng,¹ A. Denig,²² I. Denysenko,²³ M. Destefanis,^{49a,49c} F. De Mori,^{49a,49c} Y. Ding,²⁷ C. Dong,³⁰ J. Dong,^{1,a} L. Y. Dong,¹ M. Y. Dong,^{1,a} S. X. Du,⁵³ P. F. Duan,¹ E. E. Eren,^{40b} J. Z. Fan,³⁹ J. Fang,^{1,a} S. S. Fang,¹ X. Fang,^{46,a} Y. Fang,¹ L. Fava,^{49b,49c} F. Feldbauer,²² G. Felici,^{20a} C. Q. Feng,^{46,a} E. Fioravanti,^{21a} M. Fritsch,^{14,22} C. D. Fu,¹ Q. Gao,¹ X. Y. Gao,² Y. Gao,³⁹ Z. Gao,^{46,a} I. Garzia,^{21a} K. Goetzen,¹⁰ W. X. Gong,^{1,a} W. Gradl,²² M. Greco,^{49a,49c} M. H. Gu,^{1,a} Y. T. Gu,¹² Y. H. Guan,^{1,*} A. Q. Guo,¹ L. B. Guo,²⁸ Y. Guo,¹ Y. P. Guo,²² Z. Haddadi,²⁵ A. Hafner,²² S. Han,⁵¹ X. Q. Hao,¹⁵ F. A. Harris,⁴² K. L. He,¹ X. Q. He,⁴⁵ T. Held,⁴ Y. K. Heng,^{1,a} Z. L. Hou,¹ C. Hu,²⁸ H. M. Hu,¹ J. F. Hu,^{49a,49c} T. Hu,^{1,a} Y. Hu,¹ G. M. Huang,⁶ G. S. Huang,^{46,a} J. S. Huang,¹⁵ X. T. Huang,³³ Y. Huang,²⁹ T. Hussain,⁴⁸ Q. Ji,¹ Q. P. Ji,³⁰ X. B. Ji,¹ X. L. Ji,^{1,a} L. W. Jiang,⁵¹ X. S. Jiang,^{1,a} X. Y. Jiang,³⁰ J. B. Jiao,³³ Z. Jiao,¹⁷ D. P. Jin,^{1,a} S. Jin,¹ T. Johansson,⁵⁰ A. Julin,⁴³ N. Kalantar-Nayestanaki,²⁵ X. L. Kang,¹ X. S. Kang,³⁰ M. Kavatsyuk,²⁵ B. C. Ke,⁵ P. Kiese,²² R. Kliemt,¹⁴ B. Kloss,²² O. B. Kolcu,^{40b,i} B. Kopf,⁴ M. Kornicer,⁴² W. Kühn,²⁴ A. Kupsc,⁵⁰ J. S. Lange,²⁴ M. Lara,¹⁹ P. Larin,¹⁴ C. Leng,^{49c} C. Li,⁵⁰ Cheng Li,^{46,a} D. M. Li,⁵³ F. Li,^{1,a} F. Y. Li,³¹ G. Li,¹ H. B. Li,¹ J. C. Li,¹ Jin Li,³² K. Li,³³ K. Li,¹³ Lei Li,³ P. R. Li,⁴¹ T. Li,³³ W. D. Li,¹ W. G. Li,¹ X. L. Li,³³ X. M. Li,¹² X. N. Li,^{1,a} X. Q. Li,³⁰ Z. B. Li,³⁸ H. Liang,^{46,a} Y. F. Liang,³⁶ Y. T. Liang,²⁴ G. R. Liao,¹¹ D. X. Lin,¹⁴ B. J. Liu,¹ C. X. Liu,¹ F. H. Liu,³⁵ Fang Liu,¹ Feng Liu,⁶ H. B. Liu,¹² H. H. Liu,¹⁶ H. H. Liu,¹ H. M. Liu,¹ J. Liu,¹ J. B. Liu,^{46,a} J. P. Liu,⁵¹ J. Y. Liu,¹ K. Liu,³⁹ K. Y. Liu,²⁷ L. D. Liu,³¹ P. L. Liu,^{1,a} Q. Liu,⁴¹ S. B. Liu,^{46,a} X. Liu,²⁶ Y. B. Liu,³⁰ Z. A. Liu,^{1,a} Zhiqing Liu,²² H. Loehner,²⁵ X. C. Lou,^{1,a,h} H. J. Lu,¹⁷ J. G. Lu,^{1,a} Y. Lu,¹ Y. P. Lu,^{1,a} C. L. Luo,²⁸ M. X. Luo,⁵² T. Luo,⁴² X. L. Luo,^{1,a} X. R. Lyu,^{41,†} F. C. Ma,²⁷ H. L. Ma,¹ L. L. Ma,³³ Q. M. Ma,¹ T. Ma,¹ X. N. Ma,³⁰ X. Y. Ma,^{1,a} F. E. Maas,¹⁴ M. Maggiora,^{49a,49c} Y. J. Mao,³¹ Z. P. Mao,¹ S. Marcello,^{49a,49c} J. G. Messchendorp,²⁵ J. Min,^{1,a} R. E. Mitchell,¹⁹ X. H. Mo,^{1,a} Y. J. Mo,⁶ C. Morales Morales,¹⁴ K. Moriya,¹⁹ N. Yu. Muchnoi,^{9f} H. Muramatsu,⁴³ Y. Nefedov,²³ F. Nerling,¹⁴ I. B. Nikolaev,^{9f} Z. Ning,^{1,a} S. Nisar,⁸ S. L. Niu,^{1,a} X. Y. Niu,¹ S. L. Olsen,³² Q. Ouyang,^{1,a} S. Pacetti,^{20b} P. Patteri,^{20a} M. Pelizaeus,⁴ H. P. Peng,^{46,a} K. Peters,¹⁰ J. Pettersson,⁵⁰ J. L. Ping,²⁸ R. G. Ping,¹ R. Poling,⁴³ V. Prasad,¹ M. Qi,²⁹ S. Qian,^{1,a} C. F. Qiao,⁴¹ L. Q. Qin,³³ N. Qin,⁵¹ X. S. Qin,¹ Z. H. Qin,^{1,a} J. F. Qiu,¹ K. H. Rashid,⁴⁸ C. F. Redmer,²² M. Ripka,²² G. Rong,¹ Ch. Rosner,¹⁴ X. D. Ruan,¹² V. Santoro,^{21a} A. Sarantsev,^{23,g} M. Savrié,^{21b} K. Schoenning,⁵⁰ S. Schumann,²² W. Shan,³¹ M. Shao,^{46,a} C. P. Shen,² P. X. Shen,³⁰ X. Y. Shen,¹ H. Y. Sheng,¹ W. M. Song,¹ X. Y. Song,¹ S. Sosio,^{49a,49c} S. Spataro,^{49a,49c} G. X. Sun,¹ J. F. Sun,¹⁵ S. S. Sun,¹ Y. J. Sun,^{46,a} Y. Z. Sun,¹ Z. J. Sun,^{1,a} Z. T. Sun,¹⁹ C. J. Tang,³⁶ X. Tang,¹ I. Tapan,^{40c} E. H. Thorndike,⁴⁴ M. Tiemens,²⁵ M. Ullrich,²⁴ I. Uman,^{40b} G. S. Varner,⁴² B. Wang,³⁰ D. Wang,³¹ D. Y. Wang,³¹ K. Wang,^{1,a} L. L. Wang,¹ L. S. Wang,¹ M. Wang,³³ P. Wang,¹ P. L. Wang,¹ S. G. Wang,³¹ W. Wang,^{1,a} X. F. Wang,³⁹ Y. D. Wang,¹⁴ Y. F. Wang,^{1,a} Y. Q. Wang,²² Z. Wang,^{1,a} Z. G. Wang,^{1,a} Z. H. Wang,^{46,a} Z. Y. Wang,¹ T. Weber,²² D. H. Wei,¹¹ J. B. Wei,³¹ P. Weidenkaff,²² S. P. Wen,¹ U. Wiedner,⁴ M. Wolke,⁵⁰ L. H. Wu,¹ Z. Wu,^{1,a} L. G. Xia,³⁹ Y. Xia,¹⁸ D. Xiao,¹ H. Xiao,⁴⁷ Z. J. Xiao,²⁸ Y. G. Xie,^{1,a} Q. L. Xiu,^{1,a} G. F. Xu,¹ L. Xu,¹ Q. J. Xu,¹³ X. P. Xu,³⁷ L. Yan,^{46,a} W. B. Yan,^{46,a} W. C. Yan,^{46,a} Y. H. Yan,¹⁸ H. J. Yang,³⁴ H. X. Yang,¹ L. Yang,⁵¹ Y. Yang,⁶ Y. X. Yang,¹¹ M. Ye,^{1,a} M. H. Ye,⁷ J. H. Yin,¹ B. X. Yu,^{1,a} C. X. Yu,³⁰ J. S. Yu,²⁶ C. Z. Yuan,¹ W. L. Yuan,²⁹ Y. Yuan,¹ A. Yuncu,^{40b,c} A. A. Zafar,⁴⁸ A. Zallo,^{20a} Y. Zeng,¹⁸ B. X. Zhang,¹ B. Y. Zhang,^{1,a} C. Zhang,²⁹ C. C. Zhang,¹ D. H. Zhang,¹ H. H. Zhang,³⁸ H. Y. Zhang,^{1,a} J. J. Zhang,¹ J. L. Zhang,¹ J. Q. Zhang,¹ J. W. Zhang,^{1,a} J. Y. Zhang,¹ J. Z. Zhang,¹ K. Zhang,¹ L. Zhang,¹ X. Y. Zhang,³³ Y. Zhang,¹ Y. N. Zhang,⁴¹ Y. H. Zhang,^{1,a} Y. T. Zhang,^{46,a} Yu Zhang,⁴¹ Z. H. Zhang,⁶ Z. P. Zhang,⁴⁶ Z. Y. Zhang,⁵¹ G. Zhao,¹ J. W. Zhao,^{1,a} J. Y. Zhao,¹ J. Z. Zhao,^{1,a} Lei Zhao,^{46,a} Ling Zhao,¹ M. G. Zhao,³⁰ Q. Zhao,¹ Q. W. Zhao,¹ S. J. Zhao,⁵³ T. C. Zhao,¹ Y. B. Zhao,^{1,a} Z. G. Zhao,^{46,a} A. Zhemchugov,^{23,d} B. Zheng,⁴⁷ J. P. Zheng,^{1,a} W. J. Zheng,³³ Y. H. Zheng,⁴¹ B. Zhong,²⁸ L. Zhou,^{1,a} X. Zhou,⁵¹ X. K. Zhou,^{46,a} X. R. Zhou,^{46,a} X. Y. Zhou,¹ K. Zhu,¹ K. J. Zhu,^{1,a} S. Zhu,¹ S. H. Zhu,⁴⁵ X. L. Zhu,³⁹ Y. C. Zhu,^{46,a} Y. S. Zhu,¹ Z. A. Zhu,¹ J. Zhuang,^{1,a} L. Zotti,^{49a,49c} B. S. Zou,¹ and J. H. Zou¹

(BESIII Collaboration)

- ¹*Institute of High Energy Physics, Beijing 100049, People's Republic of China*
²*Beihang University, Beijing 100191, People's Republic of China*
³*Beijing Institute of Petrochemical Technology, Beijing 102617, People's Republic of China*
⁴*Bochum Ruhr-University, D-44780 Bochum, Germany*
⁵*Carnegie Mellon University, Pittsburgh, Pennsylvania 15213, USA*
⁶*Central China Normal University, Wuhan 430079, People's Republic of China*
⁷*China Center of Advanced Science and Technology, Beijing 100190, People's Republic of China*
⁸*COMSATS Institute of Information Technology, Lahore, Defence Road, Off Raiwind Road, 54000 Lahore, Pakistan*
⁹*G.I. Budker Institute of Nuclear Physics SB RAS (BINP), Novosibirsk 630090, Russia*
¹⁰*GSI Helmholtzcentre for Heavy Ion Research GmbH, D-64291 Darmstadt, Germany*
¹¹*Guangxi Normal University, Guilin 541004, People's Republic of China*
¹²*GuangXi University, Nanning 530004, People's Republic of China*
¹³*Hangzhou Normal University, Hangzhou 310036, People's Republic of China*
¹⁴*Helmholtz Institute Mainz, Johann-Joachim-Becher-Weg 45, D-55099 Mainz, Germany*
¹⁵*Henan Normal University, Xinxiang 453007, People's Republic of China*
¹⁶*Henan University of Science and Technology, Luoyang 471003, People's Republic of China*
¹⁷*Huangshan College, Huangshan 245000, People's Republic of China*
¹⁸*Hunan University, Changsha 410082, People's Republic of China*
¹⁹*Indiana University, Bloomington, Indiana 47405, USA*
^{20a}*INFN Laboratori Nazionali di Frascati, I-00044, Frascati, Italy;*
^{20b}*INFN and University of Perugia, I-06100 Perugia, Italy*
^{21a}*INFN Sezione di Ferrara, I-44122 Ferrara, Italy;*
^{21b}*University of Ferrara, I-44122 Ferrara, Italy*
²²*Johannes Gutenberg University of Mainz, Johann-Joachim-Becher-Weg 45, D-55099 Mainz, Germany*
²³*Joint Institute for Nuclear Research, 141980 Dubna, Moscow Region, Russia*
²⁴*Justus Liebig University Giessen, II. Physikalisches Institut, Heinrich-Buff-Ring 16, D-35392 Giessen, Germany*
²⁵*KVI-CART, University of Groningen, NL-9747 AA Groningen, Netherlands*
²⁶*Lanzhou University, Lanzhou 730000, People's Republic of China*
²⁷*Liaoning University, Shenyang 110036, People's Republic of China*
²⁸*Nanjing Normal University, Nanjing 210023, People's Republic of China*
²⁹*Nanjing University, Nanjing 210093, People's Republic of China*
³⁰*Nankai University, Tianjin 300071, People's Republic of China*
³¹*Peking University, Beijing 100871, People's Republic of China*
³²*Seoul National University, Seoul 151-747, Korea*
³³*Shandong University, Jinan 250100, People's Republic of China*
³⁴*Shanghai Jiao Tong University, Shanghai 200240, People's Republic of China*
³⁵*Shanxi University, Taiyuan 030006, People's Republic of China*
³⁶*Sichuan University, Chengdu 610064, People's Republic of China*
³⁷*Soochow University, Suzhou 215006, People's Republic of China*
³⁸*Sun Yat-Sen University, Guangzhou 510275, People's Republic of China*
³⁹*Tsinghua University, Beijing 100084, People's Republic of China*
^{40a}*Istanbul Aydin University, 34295 Sefakoy, Istanbul, Turkey*
^{40b}*Dogus University, 34722 Istanbul, Turkey*
^{40c}*Uludag University, 16059 Bursa, Turkey*
⁴¹*University of Chinese Academy of Sciences, Beijing 100049, People's Republic of China*
⁴²*University of Hawaii, Honolulu, Hawaii 96822, USA*
⁴³*University of Minnesota, Minneapolis, Minnesota 55455, USA*
⁴⁴*University of Rochester, Rochester, New York 14627, USA*
⁴⁵*University of Science and Technology Liaoning, Anshan 114051, People's Republic of China*
⁴⁶*University of Science and Technology of China, Hefei 230026, People's Republic of China*
⁴⁷*University of South China, Hengyang 421001, People's Republic of China*
⁴⁸*University of the Punjab, Lahore 54590, Pakistan*
^{49a}*University of Turin, I-10125 Turin, Italy*
^{49b}*University of Eastern Piedmont, I-15121 Alessandria, Italy*
^{49c}*INFN, I-10125 Turin, Italy*
⁵⁰*Uppsala University, Box 516, SE-75120 Uppsala, Sweden*
⁵¹*Wuhan University, Wuhan 430072, People's Republic of China*
⁵²*Zhejiang University, Hangzhou 310027, People's Republic of China*
⁵³*Zhengzhou University, Zhengzhou 450001, People's Republic of China*

(Received 27 July 2015; revised manuscript received 25 October 2015; published 27 January 2016)

We present a measurement of the azimuthal asymmetries of two charged pions in the inclusive process $e^+e^- \rightarrow \pi\pi X$, based on a data set of 62 pb^{-1} at the center-of-mass energy of 3.65 GeV collected with the BESIII detector. These asymmetries can be attributed to the Collins fragmentation function. We observe a nonzero asymmetry, which increases with increasing pion momentum. As our energy scale is close to that of the existing semi-inclusive deep inelastic scattering experimental data, the measured asymmetries are important inputs for the global analysis of extracting the quark transversity distribution inside the nucleon and are valuable to explore the energy evolution of the spin-dependent fragmentation function.

DOI: 10.1103/PhysRevLett.116.042001

The quark-hadron fragmentation process is parametrized with a fragmentation function (FF), which describes the probability that a hadron carrying a fraction of the parton energy is found in the hadronization debris of the fragmenting parton. The Collins FF, which considers the spin-dependent effects in fragmentation processes, was first discussed by Collins in Ref. [1]. It connects the transverse quark spin with a measurable azimuthal asymmetry (the so-called Collins effect) in the distribution of hadronic fragments along the initial quark's momentum.

The measurement of the Collins FF provides an important test in understanding strong interaction dynamics and thus is of fundamental interest in understanding QCD, the underlying theory of the strong interaction. Because of its chiral-odd nature, it needs to couple to another chiral-odd function, for instance, the transversity distribution [2–4] in semi-inclusive deep inelastic scattering (SIDIS) or another Collins FF in e^+e^- annihilations, to form accessible observables. The transversity distribution, which contributes to the nucleon transverse spin, corresponds to the tensor charge of the nucleon and is the least known leading-twist quark distribution function. There have been several SIDIS measurements of this asymmetry from HERMES [5,6], COMPASS [7], and JLab [8]. Direct information on the Collins FF can be obtained from e^+e^- annihilation experiments, as suggested in Ref. [9]. Measurements performed by the Belle [10–12] and BABAR [13] Collaborations give consistent nonzero asymmetries. Based on the universality of the involved functions in e^+e^- and SIDIS [14] experiments, global analyses [15,16] have been performed to simultaneously extract the transversity and Collins FF. However, the e^+e^- Collins asymmetries taken from Belle and BABAR correspond to considerably higher Q^2 ($\approx 100 \text{ GeV}^2$) than the typical energy scale of the existing SIDIS data (mostly 2–20 GeV^2). Therefore, the energy evolution of the Collins FF at different Q^2 is a key factor to evaluate the transversity [17]. Recently, the treatment of the evolution is developed in Refs. [18–22], which predict about a factor of 2 change in the observed asymmetries between BESIII energy and Belle and BABAR energy but is not directly validated by experimental data. The BESIII experiment [23] studies e^+e^- annihilations at a moderate energy scale (4–20 GeV^2). It is important to investigate the interesting feature of Collins FF at this energy scale, and the results can

then be connected more directly to the SIDIS. Moreover, as emphasized in Ref. [18], with significantly lower Q^2 with respect to B factories, the results will be crucial to explore the Q^2 evolution of the Collins FF and further the uncertainty of the extracted transversity, thus improving our understanding of both Collins FF and transversity.

In this Letter, we present the measurement of azimuthal asymmetries in hadron-hadron correlations for inclusive charged pion pair production $e^+e^- \rightarrow \pi\pi X$, which can be attributed to the Collins effect. The analysis is based on a data sample with an integrated luminosity of 62 pb^{-1} collected with the BESIII detector [23] at the center-of-mass energy $\sqrt{s} = 3.65 \text{ GeV}$, where the energy is away from resonances. Compared to the existing e^+e^- data, in this measurement, only fragmenting u , d , s quarks are involved. The results are free from charm contribution; as such, the combination with SIDIS data is more straightforward. The apparatus relevant to this work includes a main drift chamber (MDC), a time-of-flight system, and an electromagnetic calorimeter (EMC). Details on the features and capabilities of the BESIII detector can be found in Refs. [23,24].

Monte Carlo (MC) simulated events, which are processed with a full GEANT4-based [25] simulation of the BESIII detector, are used to optimize the event selection criteria and check for systematics. The MC samples for light quarks in $e^+e^- \rightarrow q\bar{q}$ ($q = u, d, s$) processes are generated by the LUARLW [26] package, which is based on the Lund model [27,28]. More MC samples including QED processes [$e^+e^- \rightarrow l^+l^-$ ($l = e, \mu, \tau$), $e^+e^- \rightarrow \gamma\gamma$], two photon fusion ($e^+e^- \rightarrow e^+e^-X$), line-shape tail production of $\psi(2S)$, and the initial state radiative process $e^+e^- \rightarrow \gamma J/\psi$ are analyzed to identify possible backgrounds.

Taking into account the spin of the quark, the number density $D_h^{q\uparrow}$ for finding a spinless hadron h with transverse momentum \mathbf{P}_h^\perp produced from a transversely polarized quark q with spin \mathbf{S}_q can be described in terms of the unpolarized FF D_1^q and the Collins FF $H_1^{\perp q}$ at the leading twist [29]

$$D_h^{q\uparrow}(z, \mathbf{P}_h^\perp) = D_1^q(z, \mathbf{P}_h^{\perp 2}) + H_1^{\perp q}(z, \mathbf{P}_h^{\perp 2}) \frac{(\hat{\mathbf{k}} \times \mathbf{P}_h^\perp) \cdot \mathbf{S}_q}{zM_h}, \quad (1)$$

where $\hat{\mathbf{k}}$ denotes the direction of the initial quark q , $z = 2E_h/Q$ denotes the fractional energy of the hadron relative to half of $Q = \sqrt{s}$, and M_h is the hadron mass. The second term contains the Collins FF and depends on the spin orientation of the quark q , which leads to a sine modulation of the angle spanned by \mathbf{P}_h^\perp and the plane normal to the quark spin.

In hadron production in $e^+e^- \rightarrow q\bar{q}$ events, the Collins effect can be observed when the fragments of the quark and antiquark are considered simultaneously. At $\sqrt{s} = 3.65$ GeV, due to the absent of the clear jet structure, there is no good way to estimate the $q\text{-}\bar{q}$ axis. However, the Collins asymmetries can be investigated with the azimuthal angle ϕ_0 defined as the angle between the plane spanned by the beam axis and the momentum of the second hadron (P_2), and the plane spanned by the transverse momentum p_t of the first hadron relative to the second hadron [9,30], as shown in Fig. 1.

The normalized dihadron yield is recorded as a function of ϕ_0 and can be parametrized as $a \cos(2\phi_0) + b$, with b referring to the term which is independent of ϕ_0 , and a can be written as [9,30]

$$a(\theta_2, z_1, z_2) = \frac{\sin^2\theta_2}{1 + \cos^2\theta_2} \frac{\mathcal{F}[H_1^\perp(z_1)\bar{H}_1^\perp(z_2)/M_1M_2]}{\mathcal{F}[D_1(z_1)\bar{D}_1(z_2)]}, \quad (2)$$

where \mathcal{F} denotes a convolution over the p_t . The M_1 and M_2 are the masses of the two hadrons, z_1 and z_2 are their fractional energies, and θ_2 is the polar angle of the second hadron with respect to the beam axis. \bar{D}_1 and \bar{H}_1^\perp denote FFs for antiquarks.

We reconstruct charged tracks from hits in the MDC. We require the polar angle in the laboratory frame to satisfy $|\cos\theta| < 0.93$, and the point of closest approach to the interaction vertex of e^+e^- is required to be within 1 cm in the plane transverse to the beam line and within 10 cm along the beam axis. Particle identification for charged tracks is accomplished by combining the measured energy loss (dE/dx) in the MDC and the flight time obtained from the time of flight to determine a probability $\mathcal{L}(h = K, \pi, p, e)$ for each particle (h) hypothesis. The π^\pm (K^\pm) candidates

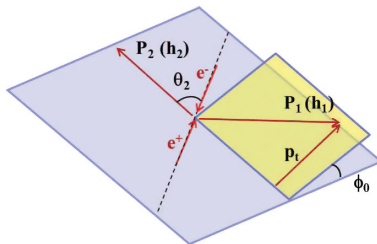


FIG. 1. The angle ϕ_0 is defined as the angle between the plane spanned by the beam axis and the momentum of the second hadron (P_2) and the plane spanned by the transverse momentum p_t of the first hadron relative to the second hadron. The angle θ_2 is the polar angle of the second hadron.

are required to satisfy $\mathcal{L}(\pi)[\mathcal{L}(K)] > 0.001$, $\mathcal{L}(\pi) > \mathcal{L}(K)$ [$\mathcal{L}(K) > \mathcal{L}(\pi)$], and $\mathcal{L}(\pi)[\mathcal{L}(K)] > \mathcal{L}(p)$. Electrons are identified with the requirement $\mathcal{L}(e) > 0.001$ and the ratio $\mathcal{L}(e)/[\mathcal{L}(e) + \mathcal{L}(\pi) + \mathcal{L}(K)] > 0.8$. Photons are reconstructed from isolated clusters in the EMC, whose energies are required to be larger than 25 MeV in the EMC barrel region ($|\cos\theta| < 0.8$) and 50 MeV in end caps ($0.84 < |\cos\theta| < 0.92$). It is required that the cluster timing delay from the reconstructed event start time does not exceed 700 ns in order to suppress electronic noise and energy deposits unrelated to the event. To select inclusive $e^+e^- \rightarrow \pi\pi X$ events, at least three charged tracks are required in order to strongly suppress two body decays. At least two of the charged tracks should be identified as pions. To suppress QED backgrounds with the final state $\tau^+\tau^-$ and unphysical backgrounds, e.g., beam-gas interactions, the visible energy in the detector, which is defined as the total energy of all reconstructed charged tracks and photons, is required to be larger than 1.5 GeV and no electron must be present in the event. Studies based on MC samples indicate that the backgrounds are suppressed to a negligible level, less than 2.5%. We select pion pairs with $z_{1(2)} \in [0.2, 0.9]$, where the lower bound is used to reduce pions originated from resonance decays (mostly ρ , f), and the upper bound is used to reject two body decays. Compared to measurement at a higher energy scale [10,13], there is no clear jet event shape at BESIII which could help to separate the hadrons coming from different fragmenting (anti)quark. Instead, to select back-to-back pions, we require the opening angle of the two charged pion candidates to be larger than 120° . This requirement reduces the possibility that two pions come from the fragmentation of the same quark. We label the two pions randomly as h_1 and h_2 , and we use the momentum direction of h_2 as a reference axis. If more than two pions are present in an event, they are combined to each other, which means each pion is allowed to be assigned to different pion pairs. In the final event selection, 331 696 events survived, which provide 557 204 available charged pion pairs.

We introduce the $2\phi_0$ normalized ratio $R = N(2\phi_0)/\langle N_0 \rangle$, where $N(2\phi_0)$ is the dipion yield in each ($2\phi_0$) subdivision and $\langle N_0 \rangle$ is the averaged bin content. The normalized ratios are built for unlike sign ($\pi^\pm\pi^\mp$), like sign ($\pi^\pm\pi^\pm$), and all pion pairs ($\pi\pi$), defined as R^U , R^L , and R^C , respectively, in which different combinations of favored FFs and disfavored FFs are involved. A favored fragmentation process refers to the fragmentation of a quark into a hadron containing a valence quark of the same flavor, for example, $u(\bar{d}) \rightarrow \pi^+$, while the corresponding $u(\bar{d}) \rightarrow \pi^-$ is a disfavored process. Since the normalized ratio R is strongly affected by detector acceptance, we use double ratios $R^U/R^{L(C)}$ (UL and UC ratios) [10,11] to extract the azimuthal asymmetries. The gluon radiation may induce a $\cos(2\phi_0)$ modulation according to Ref. [30], but it is highly suppressed at the BESIII energy scale and is independent of

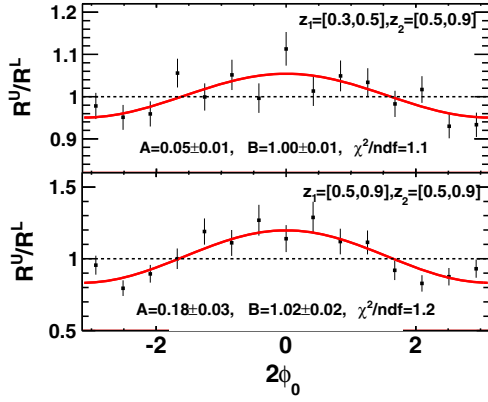


FIG. 2. Double ratio R^U/R^L versus $2\phi_0$ in the bin $z_1 \in [0.3, 0.5]$, $z_2 \in [0.5, 0.9]$ (top) and bin $z_1 \in [0.5, 0.9]$, $z_2 \in [0.5, 0.9]$ (bottom). The solid lines show the results of the fit.

the charge of the pions. Through the double ratios, charge-independent instrumental effects cancel out, and QCD radiative effects are negligible at the first order, while the charge-dependent Collins asymmetries are kept. The double ratio $R^U/R^{L(C)}$ follows the expression

$$\frac{R^U}{R^{L(C)}} = A \cos(2\phi_0) + B, \quad (3)$$

where A and B are free parameters. B should be consistent with unity, and A mainly contains the Collins effect. The A_{UL} , A_{UC} are used to denote the asymmetries for UL and UC ratios, respectively.

The analysis is performed in bins of (z_1, z_2) , p_t , and $\sin^2 \theta_2 / (1 + \cos^2 \theta_2)$. In (z_1, z_2) bins, the boundaries are set at $z_i = 0.2, 0.3, 0.5$ and 0.9 ($i = 1, 2$), where complementary off-diagonal bins (z_1, z_2) and (z_2, z_1) are combined. In each bin, normalized rates $R^{U,L,C}$ and double ratios $R^U/R^{L,C}$ are evaluated. In Fig. 2, the distributions of the double ratio R^U/R^L are shown as an example for two highest (z_1, z_2) bins with the fit results using Eq. (3). The asymmetry values (A) obtained from the fits are shown as a function of six symmetric (z_1, z_2) bins, p_t , and $\sin^2 \theta_2 / (1 + \cos^2 \theta_2)$ bins in Figs. 3 and 4, respectively. The numerical results in each (z_1, z_2) and p_t bins are listed in Table I.

Several potential sources of systematic uncertainties are investigated, and all systematic uncertainties are added in quadrature finally. An important test is the extraction of double ratios from MC samples, in which the Collins asymmetries are not included but radiative gluon and detector acceptance effects are taken into account. In the MC samples, which is about 10 times of data statistics, double ratios are found to be consistent with 0 in all bins within statistical uncertainties. To test any potential smearing effects in the reconstruction process, MC samples are reweighted to produce generated asymmetries which vary in (0.02, 0.15) for UL ratios and (0.01, 0.08) for UC ratios in different bins. The reconstructed asymmetries are

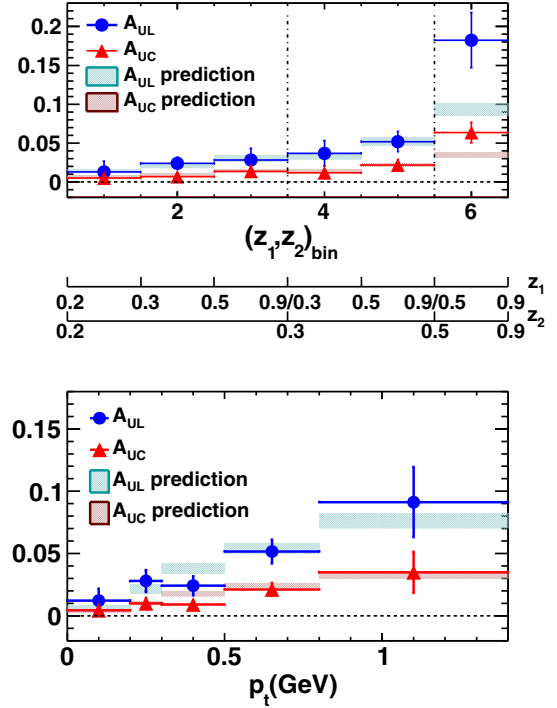


FIG. 3. Asymmetries as a function of fractional energies (z_1, z_2) (top) and p_t (bottom) for the UL (dots) and UC (triangles) ratios, where the p_t refers to the transverse momentum of the first hadron relative to the second hadron, as shown in Fig. 1. In the top figure, the lower scales show the boundaries of the bins in z_1 and z_2 . Theoretical predictions from the authors of Ref. [19] are overlaid, where the hatched areas show the predicted bands.

basically consistent with input; the differences between them, which range from 0.2% to 48% for UL ratios and range from 2% to 31% for UC ratios relatively, are included in the systematic uncertainties.

Additional possible contribution from gluon radiation can be examined in data by subtracting the normalized yields $R^U - R^{L(C)}$. The subtraction method will cancel all

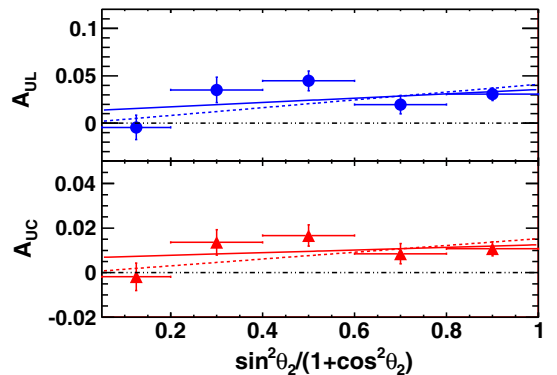


FIG. 4. Asymmetries as a function of $\sin^2 \theta_2 / (1 + \cos^2 \theta_2)$ for UL (dots) and UC (triangles) ratios. Linear fits with the constant term being set to 0 (dashed line) or a free parameter (solid line) are shown.

TABLE I. Results of A_{UL} and A_{UC} in each (z_1, z_2) and p_t bin. The uncertainties are statistical and systematic, respectively. The averages $\langle z_i \rangle$, $\langle p_t \rangle$, and $\langle \sin^2\theta_2 \rangle / \langle 1 + \cos^2\theta_2 \rangle$ are also given.

$z_1 \leftrightarrow z_2$	$\langle z_1 \rangle$	$\langle z_2 \rangle$	$\langle p_t \rangle$ (GeV)	$\langle \sin^2\theta_2 \rangle / \langle 1 + \cos^2\theta_2 \rangle$	A_{UL}	A_{UC}
[0.2,0.3][0.2,0.3]	0.245	0.245	0.262	0.589	$0.0128 \pm 0.0085 \pm 0.0114$	$0.0050 \pm 0.0038 \pm 0.0017$
[0.2,0.3][0.3,0.5]	0.311	0.311	0.329	0.576	$0.0240 \pm 0.0068 \pm 0.0042$	$0.0067 \pm 0.0032 \pm 0.0041$
[0.2,0.3][0.5,0.9]	0.428	0.426	0.444	0.572	$0.0281 \pm 0.0131 \pm 0.0077$	$0.0136 \pm 0.0064 \pm 0.0029$
[0.3,0.5][0.3,0.5]	0.379	0.379	0.388	0.563	$0.0369 \pm 0.0097 \pm 0.0132$	$0.0117 \pm 0.0046 \pm 0.0015$
[0.3,0.5][0.5,0.9]	0.498	0.499	0.479	0.564	$0.0518 \pm 0.0120 \pm 0.0049$	$0.0217 \pm 0.0056 \pm 0.0046$
[0.5,0.9][0.5,0.9]	0.625	0.628	0.499	0.570	$0.1824 \pm 0.0290 \pm 0.0204$	$0.0637 \pm 0.0118 \pm 0.0061$

p_t (GeV)	$\langle p_t \rangle$ (GeV)	$\langle z_1 \rangle$	$\langle z_2 \rangle$	$\langle \sin^2\theta_2 \rangle / \langle 1 + \cos^2\theta_2 \rangle$	A_{UL}	A_{UC}
[0.00,0.20]	0.133	0.291	0.348	0.574	$0.0122 \pm 0.0093 \pm 0.0021$	$0.0044 \pm 0.0043 \pm 0.0006$
[0.20,0.30]	0.253	0.285	0.344	0.579	$0.0279 \pm 0.0081 \pm 0.0034$	$0.0100 \pm 0.0038 \pm 0.0016$
[0.30,0.45]	0.405	0.327	0.346	0.570	$0.0241 \pm 0.0072 \pm 0.0025$	$0.0090 \pm 0.0031 \pm 0.0026$
[0.45,0.80]	0.610	0.453	0.349	0.571	$0.0516 \pm 0.0087 \pm 0.0040$	$0.0211 \pm 0.0049 \pm 0.0019$
[0.80,1.40]	0.923	0.646	0.334	0.584	$0.0913 \pm 0.0249 \pm 0.0133$	$0.0350 \pm 0.0116 \pm 0.0116$

the radiative terms, but the cancellation of the acceptance effects may be incomplete. The differences between the asymmetries obtained with the subtraction method and the nominal results range from 0.001 to 0.01 for UL ratios and from 0.0 to 0.005 for UC ratios. These are assigned as absolute systematic uncertainties.

The probability of misidentifying kaons as pions may introduce $K\pi$ pairs and KK pairs into the $\pi\pi$ samples of interest. However, due to the much lower inclusive production cross section for charged kaons compared to pions, the $\pi\pi$ asymmetry receives non-negligible contribution only from the $K\pi$ combination. We denote with $A^{\pi\pi}$ and $A^{K\pi}$ the corresponding Collins asymmetries in data. They can be obtained by unfolding the measurements of $A_{\text{mea}}^{\pi\pi}$ and $A_{\text{mea}}^{K\pi}$, where $A_{\text{mea}}^{\pi\pi} = (1 - f_{K\pi})A^{\pi\pi} + f_{K\pi}A^{K\pi}$, $A_{\text{mea}}^{K\pi} = (1 - f_{\pi\pi})A^{K\pi} + f_{\pi\pi}A^{\pi\pi}$, $f_{K\pi}$, and $f_{\pi\pi}$ are the MC-determined contamination fractions. Depending on the (z_1, z_2) bin, $f_{K\pi}$ is found to range from 0.0% to 4.5% and $f_{\pi\pi}$ ranges from 0.1% to 35.4%. The errors on $A^{K\pi}$ are very large, and the changes in $A^{\pi\pi}$ from the nominal values are in (0.001, 0.005) for UL ratios and (0.0, 0.001) for UC ratios, and are assigned as systematic uncertainty.

Additional higher harmonic terms (such as $\sin 2\phi_0$ and $\cos 4\phi_0$) are also included in the fit function to validate the robustness of the fit. The changes of the value of the cosine asymmetries, which vary in (0.001, 0.009) for UL ratios and (0.0, 0.003) for UC ratios, are included in the systematic uncertainties.

We have also verified null asymmetries for the double ratio of $\pi^+\pi^+/\pi^-\pi^-$ pairs and for random combinations of pairs of tracks from different events. From these tests, no significant asymmetries are observed. The beam polarization may contribute to the measured asymmetries. We study the angular distribution of the $e^+e^- \rightarrow \mu^+\mu^-$ process, which is sensitive to beam polarization. No buildup of polarization is observed.

Adding statistical and systematic uncertainties in quadrature, we observe significant, nonzero Collins asymmetries, as shown in Fig. 3. These asymmetries rise with fractional energies and p_t as expected theoretically [9] and seen in higher-energy e^+e^- experiments [10–13]. The predictions of authors of Ref. [19], based on results from previous data and the energy evolution model, are also shown in Fig. 3 and are basically consistent with our results. A direct comparison with higher-energy e^+e^- data is meaningless due to differing kinematics. However, asymmetries in our data are 1.5 times higher overall and higher by 0–2 sigma at points of comparable z and p_t .

The expected behavior of the Collins asymmetries as a function of $\sin^2\theta_2/(1 + \cos^2\theta_2)$ is linear and vanishes at $\theta_2 = 0$, as formulated in Eq. (2). Thus, a linear fit is performed to the points in Fig. 4, with the constant term set to be 0 or left as a free parameter, which gives the reduced χ^2 to be 2.3 or 2.8 for A_{UL} and 1.7 or 1.9 for A_{UC} , respectively. The significance for a zero offset is only about 1σ for both A_{UL} and A_{UC} .

The authors of the very recent paper Ref. [19] give the theoretical predictions for the BESIII energy scale, which are also shown in Fig. 3. Overall, our measured asymmetries are compatible with those predictions, except at the largest z interval.

In summary, we perform a measurement of the azimuthal asymmetry in the inclusive production of charged pion pairs. Our results suggest nonzero asymmetry in the region of large fractional energy z , which can be attributed to the product of a quark and an antiquark Collins function. This is the first measurement of the Collins asymmetry at low energy scale ($Q^2 \approx 13 \text{ GeV}^2$) in e^+e^- annihilation. The observed asymmetry indicates a larger spin-dependent Collins effect than those at the higher energy scale from B factories [10–13]. The results are of great importance to explore the Q^2 evolution of the Collins function and extract transversity distributions in nucleon.

The authors would like to thank D. Boer, X. D. Jiang, J. P. Ma, P. Sun, and F. Yuan for helpful discussions on the theoretical aspects of the measurement. The BESIII Collaboration thanks the staff of BEPCII and the IHEP computing center for their strong support. This work is supported in part by National Key Basic Research Program of China under Contract No. 2015CB856700; National Natural Science Foundation of China (NSFC) under Contracts No. 11125525, No. 11235011, No. 11275266, No. 11322544, No. 11335008, and No. 11425524; the Chinese Academy of Sciences (CAS) Large-Scale Scientific Facility Program; the CAS Center for Excellence in Particle Physics (CCEPP); the Collaborative Innovation Center for Particles and Interactions (CICPI); Joint Large-Scale Scientific Facility Funds of the NSFC and CAS under Contracts No. 11179007, No. U1232201, and No. U1332201; CAS under Contracts No. KJCX2-YW-N29 and No. KJCX2-YW-N45; 100 Talents Program of CAS; National 1000 Talents Program of China; INPAC and Shanghai Key Laboratory for Particle Physics and Cosmology; German Research Foundation DFG under Contract No. Collaborative Research Center CRC-1044; Istituto Nazionale di Fisica Nucleare, Italy; Ministry of Development of Turkey under Contract No. DPT2006K-120470; Russian Foundation for Basic Research under Contract No. 14-07-91152; The Swedish Research Council; U.S. Department of Energy under Contracts No. DE-FG02-04ER41291, No. DE-FG02-05ER41374, No. DE-FG02-94ER40823, and No. DESC0010118; U.S. National Science Foundation; University of Groningen (RuG) and the Helmholtzzentrum fuer Schwerionenforschung GmbH (GSI), Darmstadt; WCU Program of National Research Foundation of Korea under Contract No. R32-2008-000-10155-0.

*Corresponding author.
guanyh@ihep.ac.cn

†Corresponding author.
xiaorui@ucas.ac.cn

^aAlso at State Key Laboratory of Particle Detection and Electronics, Beijing 100049, Hefei 230026, People's Republic of China.

^bAlso at Ankara University, 06100 Tandogan, Ankara, Turkey.

^cAlso at Bogazici University, 34342 Istanbul, Turkey.

^dAlso at the Moscow Institute of Physics and Technology, Moscow 141700, Russia.

^eAlso at the Functional Electronics Laboratory, Tomsk State University, Tomsk 634050, Russia.

^fAlso at the Novosibirsk State University, Novosibirsk 630090, Russia.

^gAlso at the NRC “Kurchatov Institute,” PNPI, 188300 Gatchina, Russia.

^hAlso at University of Texas at Dallas, Richardson, TX 75083, USA.

ⁱAlso at Istanbul Arel University, 34295 Istanbul, Turkey.

- [1] J. C. Collins, *Nucl. Phys.* **B396**, 161 (1993).
- [2] J. P. Ralston and D. E. Soper, *Nucl. Phys.* **B152**, 109 (1979).
- [3] R. L. Jaffe and X.-D. Ji, *Phys. Rev. Lett.* **67**, 552 (1991).
- [4] R. L. Jaffe and X.-D. Ji, *Nucl. Phys.* **B375**, 527 (1992).
- [5] A. Airapetian *et al.* (HERMES Collaboration), *Phys. Rev. Lett.* **94**, 012002 (2005).
- [6] A. Airapetian *et al.* (HERMES Collaboration), *Phys. Lett. B* **693**, 11 (2010).
- [7] C. Adolph *et al.* (COMPASS Collaboration), *Phys. Lett. B* **717**, 376 (2012).
- [8] X. Qian *et al.* (Jefferson Lab Hall A Collaboration), *Phys. Rev. Lett.* **107**, 072003 (2011).
- [9] D. Boer, R. Jakob, and P. J. Mulders, *Nucl. Phys.* **B504**, 345 (1997).
- [10] R. Seidl *et al.* (Belle Collaboration), *Phys. Rev. Lett.* **96**, 232002 (2006).
- [11] R. Seidl *et al.* (Belle Collaboration), *Phys. Rev. D* **78**, 032011 (2008).
- [12] R. Seidl *et al.* (Belle Collaboration), *Phys. Rev. D* **86**, 039905(E) (2012).
- [13] J. P. Lees *et al.* (BABAR Collaboration), *Phys. Rev. D* **90**, 052003 (2014).
- [14] A. Metz, *Phys. Lett. B* **549**, 139 (2002).
- [15] M. Anselmino, M. Boglione, U. D'Alesio, S. Melis, F. Murgia, and A. Prokudin, *Phys. Rev. D* **87**, 094019 (2013).
- [16] A. Martin, F. Bradamante, and V. Barone, *Phys. Rev. D* **91**, 014034 (2015).
- [17] Z.-B. Kang, A. Prokudin, P. Sun, and F. Yuan, *Phys. Rev. D* **91**, 071501 (2015).
- [18] P. Sun and F. Yuan, *Phys. Rev. D* **88**, 034016 (2013).
- [19] Z.-B. Kang, A. Prokudin, P. Sun, and F. Yuan, *Phys. Rev. D* **93**, 014009 (2016).
- [20] F. Yuan and J. Zhou, *Phys. Rev. Lett.* **103**, 052001 (2009).
- [21] Z.-B. Kang, *Phys. Rev. D* **83**, 036006 (2011).
- [22] K. Kanazawa and Y. Koike, *Phys. Rev. D* **88**, 074022 (2013).
- [23] M. Ablikim *et al.* (BESIII Collaboration), *Nucl. Instrum. Methods Phys. Res., Sect. A* **614**, 345 (2010).
- [24] C. Zhang, *Sci. China G* **53**, 2084 (2010).
- [25] S. Agostinelli *et al.* (GEANT4 Collaboration), *Nucl. Instrum. Methods Phys. Res., Sect. A* **506**, 250 (2003).
- [26] H.-M. Hu and X.-Y. Li, *Int. J. Mod. Phys. A* **24**, 111 (2009).
- [27] J. C. Chen, G. S. Huang, X. R. Qi, D. H. Zhang, and Y. S. Zhu, *Phys. Rev. D* **62**, 034003 (2000).
- [28] T. Sjostrand, *Comput. Phys. Commun.* **27**, 243 (1982).
- [29] A. Bacchetta, U. D'Alesio, M. Diehl, and C. A. Miller, *Phys. Rev. D* **70**, 117504 (2004).
- [30] D. Boer, *Nucl. Phys.* **B806**, 23 (2009).